Wavefront and distance measurement using the CAFADIS camera.

J.M. Rodríguez-Ramos*[a], B. Femenía Castellá[b], F. Pérez Nava[a] , S. Fumero[a]

[a]University of La Laguna, Avda. Fco. Sánchez s/n, 38202, La Laguna, Spain
[b]Grantecan, C/ Vía Láctea S/N, 38200, La Laguna, Spain;

ABSTRACT

The CAFADIS camera is a new sensor patented by Universidad de La Laguna (Canary Islands, Spain): international patent PCT/ES2007/000046 (WIPO publication number WO/2007/082975). It can measure the wavefront phase and the distance to the light source at the same time in a real time process. This could be really useful when using Adaptive Optics with Laser Guide Stars, in order to know the LGS height variations during the observation, or even the 3D LGS profile at Na layer .

The CAFADIS camera has been designed using specialized hardware: Graphical Processing Units (GPUs) and Field Programmable Gates Arrays (FPGAs). These two kinds of electronic hardware present an architecture capable of handling the sensor output stream in a massively parallel approach. Previous papers have shown their ability for AO in ELTs.

CAFADIS is composed, essentially, by a microlenses array at the telescope image space, sampling the image instead of the telescope pupil. Conceptually, when only 2x2 microlenses are presented it is very similar to the pyramid sensor. But in fact, this optical design can be used to measure distances in the object space using a variety of techniques.

Our paper shows a simulation of an observation using Na-LGS and Raylegh-LGS at the same time, where both of the LGS heights are accurately measured. The employed techniques are presented and future applications are introduced.

Keywords: Adaptive optics, LGS, wavefront phase recovery, plenoptic sensor, depths, GPU, FPGA.

1. INTRODUCTION

In view of the very large diameter telescopes currently in operation (GRANTECAN, Keck, etc), and future giant telescopes (30 to 40 metres in diameter) adaptive optics (AO) is an essential key in order to gain not only in photon collection capabilities (due to the increase of aperture size) but also in spatial resolution as it would be the case if not atmospheric turbulence affected astronomical observations. In addition to classical AO, a large number of science cases request the possibility of having the AO correction over Fields Of View much larger that simply the isoplanatic patch provided by single conjugate AO systems which are of the order of a few arcsecs in the visible. Such an increase in the area corrected by AO can be achieved by measuring the 3D distribution of the atmospheric phase (i.e. tomography) and control several correcting devices (i.e. deformable mirrors) conjugated at different heights in the atmosphere, that is, performing multi-conjugate adaptive optics (MCAO). At present, all the current MCAO programs aim at correcting, at best, three horizontal turbulence layers and taking into account that in order to conduct 3D atmospheric turbulence sensing with current tomographic techniques one needs more stars than layers to be corrected it is easy to realize the need of having access to several guide stars for the MCAO system. That is, it scans a minute portion of the 3D cylinder affecting the image, recovering phase estimates after extremely complex calculations, so much so that they seriously undermine adaptive correction of the optical beam within atmosphere stability time in the visible (10 ms).

*jmramos@ull.es; phone +34 922 318 249; fax +34 922 318 228;

On the other hand, the absence in the sky of a sufficient number of natural point sources calls for the use of artificial point sources: Na stars (at an altitude of 90 Km) either in the case of mono-conjugate or multi-conjugate adaptive optics cases. To generate an artificial Laser Guide Star (LGS) a very high resolution, high powered, pulsed laser is required, so the cost of this technology is gargantuan and even higher in the case of an MCAO system resorting to several LGSs. simultaneous measurements).

The camera we propose for conducting tomographical 3D spatial object measurements entails one single Shack-Hartmann sensor, assembled at the image space of a converging lens. This scheme allows obtaining sufficient data for recovery of the 3D environment with one sole measure (i.e. one single exposure). The image resulting from application of this sensor can be seen as formed by four dimensions: two CCD co-ordinates associated to the inside of each micro-lens and a further two co-ordinates stemming from the micro-lens array. The subsequent data processing technique can be undertaken in two different ways depending on the final objective: wavefront phase sensing or object distance. In the case of Adaptive Optics using Na Laser Guide Stars, the simultaneous processing is self-complemented because of the LGS elongated form: Na object profile knowledge allows defocus correction in real time.

Then, CAFADIS is composed, essentially, by a microlenses array at the image space of the telescope. Clarke and Lane[1] (2005) sampled the image at telescope focus, instead of the telescope pupil, and showed it is possible to recover the atmospheric wavefront phase at pupil. They concluded that, conceptually, when only 2x2 microlenses are presented it is very similar to the pyramid sensor. We present at this conference that phase reconstruction implemented in real time using Field Programmable Gates Arrays (J.M. Rodríguez-Ramos *et al*. [2] , 2008).

But important considerations must be done in relation to this optical design:

- This sensor corresponds to the Adelson and Wang[3] plenoptic camera (1992), and it can be used to measure distances in the object space using a variety of techniques. Ren Ng[4] (2005) have presented a wide study of the sensor, but only in order to refocus images without atmospheric turbulence considerations. More recently, we have developed a new technique for distance measuring associated to this sensor (J. M. Rodríguez-Ramos[5], (2008)) that improves resolution and reduces time processing. The resolution in distances depends on number of pixels inside of each microlens.

- In terms of wavefront sensing, the Shack-Hartmann sensor samples the telescope pupil and the pyramid sensor samples the telescope focus; but the plenoptic sensor, in fact, is an intermediate between both of them. The plenoptic sampling can be done in several image space positions, not only at focus, conjugated to the associated object image positions. The final image resolution depends on number of microlenses, and the final wavefront resolution depends on number of pixels inside of each microlens (the same as in distance resolution). Using much more than only 2x2 microlenses the pupil is sampled from different points of view, without spatial frequency lost, and extended objects or several LGS can be observed at the same time and tomographical reconstruction undertaken. We are talking about suppressing the several Shack-Hartman conjugated to each height or to each adaptive mirror.

Our technique (i) will allow stick to one sole measurement, with a single sensor, within each atmospheric stability time-slot; (ii) will allow recovery of the phase associated to each turbulent horizontal layer, i.e. tomography of the entire atmosphere, using a technique whose computational bottle-neck lies in performing multi-dimensional Fourier transforms, but for this side of our research we already have implementations that are seven times faster than FFTW in high-level CPUs;(iii) will correct from defocus measuring the elongated LGS 3D-profile in real time.

This article presents conceptual understanding of the CAFADIS camera, wavefront and distances recoveries using a simulation of the CAFADIS camera, and future applications for adaptive optics in giants telescopes.

2. CAFADIS CAMERA: CONCEPTS.

Left panel in Figure 1 shows an scheme of the CAFADIS camera optical design. It is composed of a main lens, a microlens array and a CCD. The microlens array separates the converging rays into an image on the CCD behind it. This arrangement can obtain the focal stack associated to the object space volume.

To introduce the continuous focal stack transform we parameterize the lightfield defined by all the light rays inside a camera. We will use the two-plane parameterization of this lightfield and write $L_F(\boldsymbol{x},\boldsymbol{u})$ as the radiance travelling from

position $\boldsymbol{u}=(u1,u2)'$ (apostrophe mean transpose) on the lens plane to position $\boldsymbol{x}=(x1, x2)'$ on the sensor plane. F is the distance between the lens and the sensor (see right panel Figure 1).

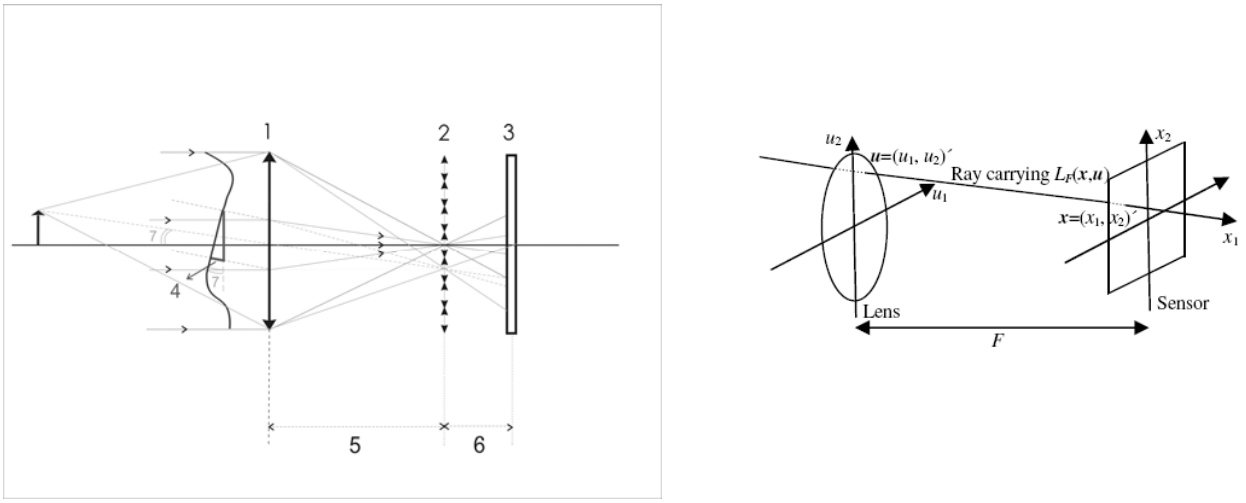

Fig. 1. LEFT PANEL: CAFADIS óptical design. 1.- represents the telescope, 2.- a microlenses array is placed at the image space, 3.- the CCD detector, 4.- wavefront phase, 5.- distance between objective lens and microlenses array plane, and 6.- microlens focal distance. RIGHT PANEL: Two plane parameterization of the lightfield.

The lightfield L_F can be used to compute conventional photographs at any depth αF. Let P_α be the operator that transforms a lightfield L_F at a sensor depth F into a photograph formed on a film at sensor depth αF, then we have:

$$\mathcal{P}_\alpha[L_F](\boldsymbol{x}) = \frac{1}{\alpha^2 F^2}\int L_F\left(\boldsymbol{u}\left(1-\frac{1}{\alpha}\right)+\frac{\boldsymbol{x}}{\alpha},\boldsymbol{u}\right)d\boldsymbol{u}.$$

This equation explains how to compute photographs at different depths from the lightfield L_F. When we compute the photographs for every sensor depth αF we obtain the focal stack transform S of the lightfield.

$$\mathcal{S}[L_F](\boldsymbol{x},\alpha) = \mathcal{P}_\alpha[L_F](\alpha\boldsymbol{x}).$$

We widely explain the depth extraction from the focal stack in Pérez Nava *et al*.[5] (2008). After the focal stack is computed, two steps must be acomplished: first step is applying a focus quality operator to estimate correctly the depth planes, and second step is computing the estimated distances using the Markov Random Field formalism.

3. SIMULATION DESIGN AND PARAMETERS

The first application for the plenoptic concept we have thought of for its immediate use in astronomical adaptive optics is the simultaneous measurement of distances and wavefront phase from an LGS. It is well known that besides the tip-tilt indetermination from the LGS (unless exotic techniques such as the polychromatic LGS scheme are adopted), Na LGS-based adaptive optics systems suffer from low-frequency defocus indetermination due to height drifts of the mesospheric Na layer. This problem is well known in today's 10-m class telescopes incorporating Na-LGS based AO systems and a series of different strategies have been adopted:

- The Na-LGS A system at Keck telescope (Summers *et al*.[6] (2004)) incorporates a Low-Bandwidth WaveFront Sensor (LBWFS) which is, in essence, a replica of the main WaveFront Sensor (WFS) but working at a much lower temporal frequency. The rationale of the LBWFS is to measure defocus and other low-order aberration modes over long time periods that are associated to drifts of the Na layer. Additionally, the LBWFS provides updates for the calibration of the quad-cells in the LGS WFS.

- The ESO VLT solution (Kasper *et al*.[7] (2004)) relies on an appropriate low temporal filtering of the defocus commands sent to the Deformable Mirror (DM). To work effectively, an initial estimate of the Na layer is required, and such an estimate is obtained from a modification of the classical LIDAR (LIght Detection And Ranging). Subsequent changes in the height of the LGS spot can be obtained from the filtered defocus commands sent to the DM.

- The Gemini North solution (Herriot *et al*.[8] (1998)) is, to our knowledge, the only AO system implementing a dedicate WFS for NGS operation and a dedicate WFS for LGS operation although both WFS share part of the same optical path within the WFS arm. Any instrument receiving light from Altair (i.e. the AO system at Gemini North telescope) is equipped with an OIWFS that is a 2×2 SH WFS from which the AO control system extracts information on tip-tilt and focus (Herriot *et al*. .[8] (1998)). This information is blended with the tip-tilt and focus information obtained from the high-order WFS when using NGS. Initial plans for the LGS upgrade in Altair were using the OIWFS to control the tip-tilt and focus, but after commissioning the Altair system in the NGS mode, the system was modified in order to use a STRAP unit for the tip-tilt sensing.

- Currently the Subaru AO system is undergoing an upgrade of its old low-order 36-element curvature WFS to build a new high-order system with 188-element curvature WFS with plans to an upgrade to LGS operation shortly after NGS comission (Watanabe *et al*.[9] (2004)). In the LGS mode, the visible spectrum outside the Na band is sent to a low-order 2×2 Shack-Hartmann WFS for tip-tilt and slow defocus sensing.

- The GTCAO system at the GTC telescope recently passed its Advanced Design Review. The WFS is being designed (Sánchez-Blanco[10] (2007)) taking into account an upgrade to LGS operation and the solution proposed is a blend of the solutions adopted for the Gemini system and Subaru in the sense that implements a dedicated WFS for LGS operation and converts the NGS WFS into a a low-order 2×2 Shack-Hartmann WFS for tip-tilt and slow defocus sensing by replacing the nominal 20×20 lenslet array in the NGS WFS with a 2×2 lenslet array.

As argued in Herriot *et al*.[11] (2006), if the Na layer drift poses a problem for the current LGS-based AO systems in 8-10m class telescopes, for the next generation of 30-40 m class telescopes the problem becomes exceptionally severe since the uncertainty Δh in the focusing distance to the Na layer translates into a rms wavefront error σ, averaged over the aperderture D, according to the expression:

$$\sigma = \frac{1}{8\sqrt{3}}\left(\frac{D}{h}\right)^2 \Delta h$$

where h is the instantaneous density-weighted mean height of the mesospheric Na layer. Plugging a few numbers into this equation reveals that for a 10-m class telescope such as GTC we expect σ=1.2 nm (D=11.4 m, h=87.5 Km) per meter of focusing distance to h, while for the proposed E-ELT σ=16.6 nm (D=42 m, h=87.5 Km) per every meter change of h. In addition, current systems in 10-m class telescopes assume that drift changes occur at long enough scales to be efficiently filtered out as done in the VLT and Keck approaches. As argued by Davis *et al*. [12] (2006), such assumption is based on the extrapolation of LIDAR measurements that are only able to sample the low-frequency range of the Na layer variability PSD. Extrapolation of this low frequency range of PSD to higher frequencies indicate the filtering of low temporal defocus for the case of an 8-10 m class telescope may be affordable. However, the same extrapolation already indicates the variability residual of such filtering for a 30-42 m class telescope would already result in a severe error source.

With this is mind we believe the plenoptic sensor (CAFADIS camera) can be of interest as it implements both the wavefront sensing form the LGS and simultaneously an accurate enough measurement of the distance to the Na LGS with two great advantages with respect to other approaches:

1. The plenoptic concept does not need an absolute defocus reference as required in the implementation of the LIDAR approach in the VLT telescopes (Kasper *et al*.[7] (2004)) or the proposed scheme by Herriot *et al*.[11] (2006) for the TMT relying on relying on the use of a NGS for the defocus distance. To be fair, it should be noticed that, however, any LGS-based AO system still requires observation of a NGS for the determination of the tip-tilt modes unless using a polychromatic LGS, but this solution seems not feasible in a short-time given

the added complexity of such systems for extra-large aperture telescope plus the fact that with large apertures the focus tip-tilt anisoplanatism will become a relevant source of error so that the absolute determination of the tip-tilt from a LGS may be not enough for tip-tilt correction of a celestial target. In this case, not using NGS for the defocus determination, as with the case of the plenotptic concept, allows the whole use of the NGS to be devoted to tip tilt determination yielding a largersky coverage.

2. The plenoptic concept incorporates simultaneous measurement of wavefront from the LGS and focusing distance to the LGS without requiring any extra hardware. Indeed, the hardware implementation of a plenoptic sensor involves, at least conceptually, even a lower degree of complexity as required by a standard Shack-Hartmann sensor as it is not required to place the lenslet array in a collimated beam.

With all these possible advantages in mind we decided to launch a simple numerical simulation to study the feasibility of simultaneous measurement of wavefront from the LGS and height determination of the LGS using the plenoptic approach. The simulation uses part of the CAOS software (Carbillet *et al.*[13] (2005)) to generate the atmospheric turbulence and perform the geometrical propagation of light through the turbulent atmosphere. In this toy simulation we restrict to a medium size telescope with D=4.2m and rather than a single elongated LGS we assume two point-like LGS located at 90 Km and at 30 Km from the entrance pupil. This would be equivalent to having available a Rayleigh beacon and a Na beacon for the 30 Km and 90 Km Lgs, respectively. An on-going simulation project aims at showing the feasibility of the plenoptic concept exploiting the extended nature of the elongated sodium beacon. Notice that unlike traditional wavefront sensors which in general degrade their performances, the nature of the plenoptic sensor exploits the extended nature of the object and in particular its focus depth. The CAFADIS camera is focused to an intermediate distance of 45 Km with respect to the entrance pupil in order to minimize the simultaneous defocus on the images of each LGSs. Both LGSs are on-axis in this toy simulation where we assume a 32x32 lenslet array with each lenlest probing a FoV of 27.7 arcsec, sampled each lenslet image with 32×32 pixels. In the figures below, the images of the LGSs are separated to help visualize them.

As we are assuming operation with LGSs, the simulation is only ran at a single wavelength of 550 nm. The interested reader is referred to the work by Clare and Lane[1] (2005) for the derivation of the following expression accounting for the image intensity on the CCD at the lenslet array focal plane given by a single lenslet:

$$I(\xi,\eta) \propto \left| h(\xi,\eta) \otimes P(\xi,\eta) \exp\left[j\phi(\xi,\eta) \right] \right|^2$$

where (ξ,η) are the coordinates on the CCD detector, $h(\xi,\eta) = FT\left[H(u,v) \right]$ is the Fourier Transform (FT) of the aperture function of a lenslet and (u,v) are the coordinates on the lenslet aperture plane, $P(x,y)$ is the telescope aperture plane, $\phi(x,y)$ is the wavefront phase on the telescope aperture containing not only the atmospheric turbulence induced phase aberration but also the defocus due to the fact the lenslet array is not conjugated to each LGS plane but at an intermediate plane. Following Clare and Lane[1] (2005), assuming square lenses in the lenslet array we arrive to the closed expression for the intensity provided by lens (m,n) within the lenslet array:

$$I_{m\,n}(\xi,\eta) \propto \left| \Delta u \frac{\sin(\pi \xi \Delta u)}{\pi \xi \Delta u} \exp\left[j2\pi \xi u_m' \right) \right] \Delta v \frac{\sin(\pi \eta \Delta u)}{\pi \eta \Delta u} \exp\left[j2\pi \eta v_n' \right) \right] \otimes P(\xi,\eta) \exp\left[j\phi(\xi,\eta) \right] \Bigg|^2$$

where $\Delta u \times \Delta v$ is the linear dimension of the (m,n) lenslet centered at coordinates (u_m', v_n'). Further on, in our simulations we also have the effect the CCD plane is discrete. Figure 2 shows the image formed in the CCD of the simulated CAFADIS configuration. In our simulation the atmospheric turbulence is introduced at a single infinitely thin layer located at 3500 m above the telescope pupil entrance and it corresponds to Kolmogrov turbulence with a Fried parameter $r_0(500nm) = 0.2m$. Figure 3 shows the wavefront at the pupil entrance arriving from each of the two LGSs where the difference between both wavefronts is shown in the right most panel and it is due exclusively to the fact that

the light from the 90 Km LGS goes through a different turbulence volume than the light from the 30 Km LGS, i.e. different cone effects for each of the LGSs.

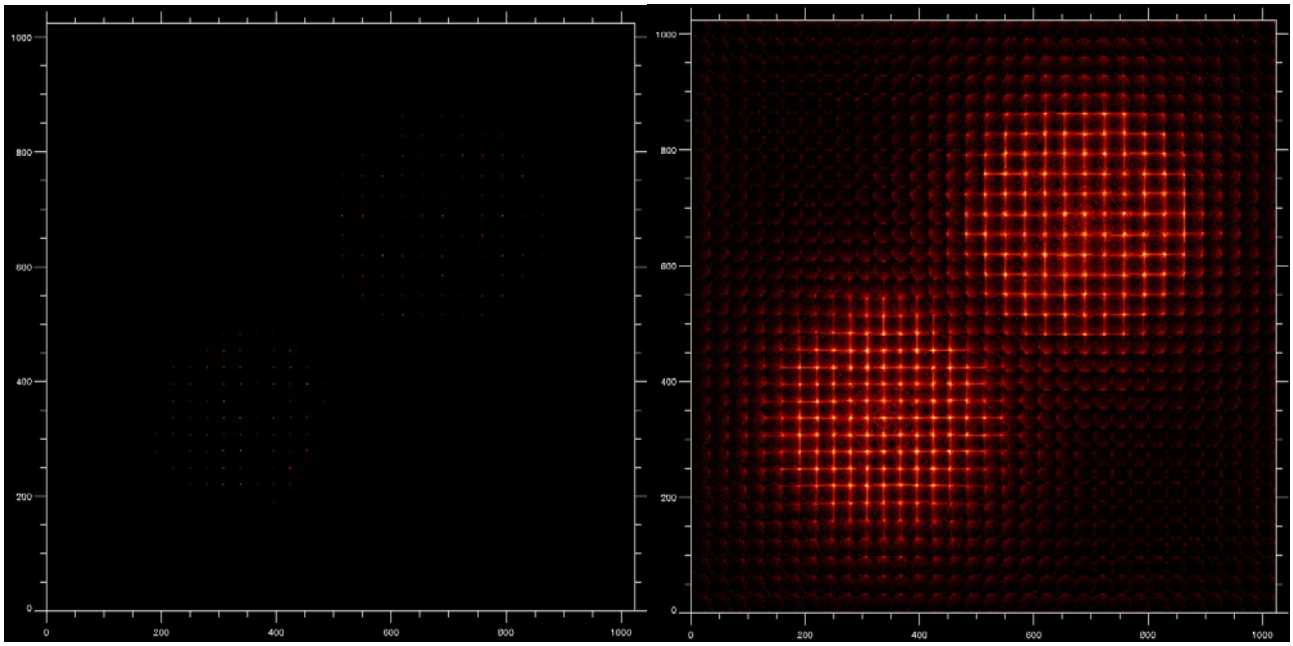

Fig. 2. Image delivered by the plenoptic setup. Left linear strecht of the image where we barely see each spot produced. Right: same image in log strecht to help visualize the structure within the image.

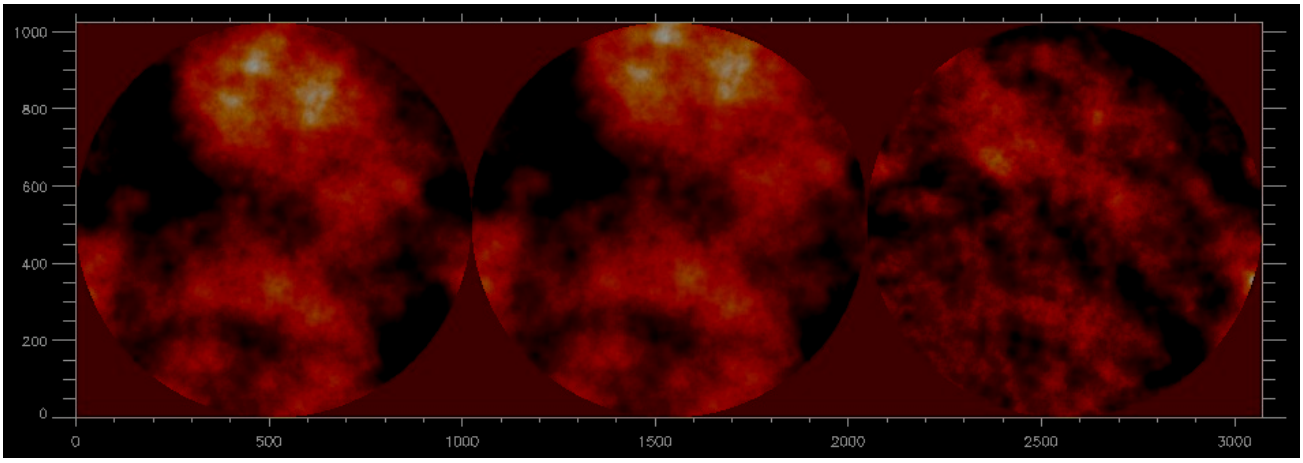

Fig. 3. Input wavefront from each of the two LGS at 90 Km (left panel) and 30 Km (central panel). Right panel shows the difference between the two inpute wavefronts.

4. WAVEFRONT RESULTS.

Applying the wavefront phase recovery algorithm to the simulation data, as described in Rodríguez-Ramos *et al.*[2] (2008) the atmospherical wavefront phase map composed at telescope pupil can be obtained from the CAFADIS camera image. Figure 4 shows the atmospherical wavefront phase reconstruction. We do not present here any qualitative analysis of the algorithm, a deep study will be published soon. What we present at this conference is a fast virtex-4 FPGA implementation of the total algorithm involved using really high samplings (Rodríguez-Ramos *et al.*[2] (2008)). The spent times are less than the atmospheric characteristic time even in a 256x256 microlenses sampling.

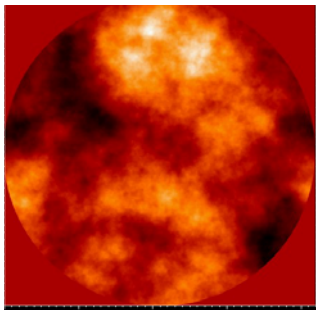

Fig. 4. Recovered atmospherical wavefront phase at telescope pupil.

5. DISTANCE RESULTS

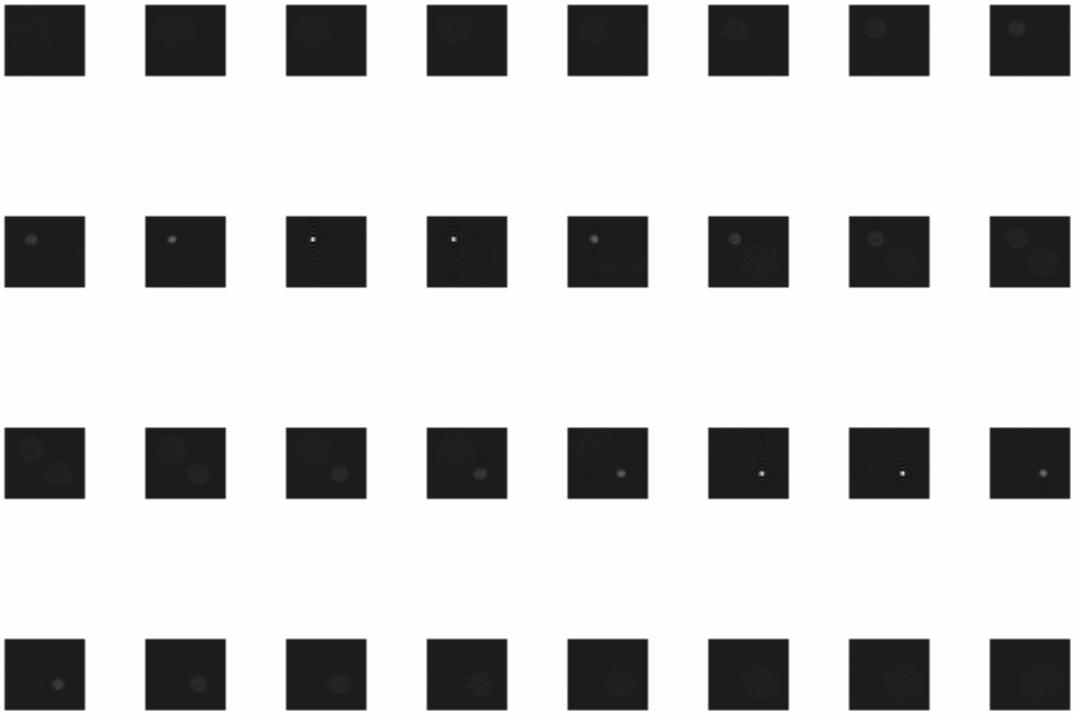

Fig. 5. Focal stack sequence of the laser guide stars simulation. From left to right and top to bottom, the atmospheric volume is shown from the bottom atmosphere to the top one. Focused Raleygh star is observed at 30 km. height, then 60 km. empty atmosphere, and finally the Na LGS at 90 km. height.

As we explained in section 3, in order to obtain the distances, the first step consists in making the focal stack calcule. Figure 5 shows the focal stack sequence associated to simulated data. This is acomplished using our new technique called Summation of Constrained Planes in an Hypercube (SCPH), see Rodríguez-Ramos *et al*.[5] (2008). This is done in a real time in our GPU implementation, thanks to a O(N) fast algorithm where fastest implementation from other authors required O(N log N). Additionally, our method requires only sums and can be parallelized to be carried out in different processors with a minimum interchange of data. For example, a 4096x4096 input problem can be done using just 1 GPU in 135 ms. For a 1024x1024 input size, computation requirements decrease in the same factor than the problem, that is a 16x reduction. Moreover our implementation performance is actually memory bound, not computationally bound (Marichal-Hernandez *et al.*[14] (2008)).

The second step for distance recovery is applying a focus quality operator (variance, laplacian,…) to estimate correctly the depth planes. In the third and last step we compute the optimal estimated distances using the Markov Random Field formalism. Figure 6 shows the results for our two laser guide stars simulation. The Raleygh star was placed at 30 km. height, and the Na laser guide star at 90km height. The microlenses array was conjugated to an intermediate point in height between both stars. The distances are correctly estimated from this middle point: the distance to the Rayleigh star appears as negative signed and the distance to the Na star as positive, as expected.

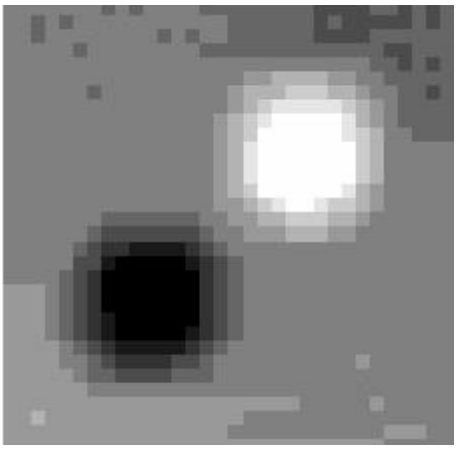

Fig. 6. The two laser guide stars distance recovery. The microlenses array was conjugated to an intermediate point between the artificial stars. This is because the distances are opposite signed: negative to the Raleygh star and positive to the Na LGS.

6. CONCLUSION AND FUTURE WORK

We present here a new wavefront phase design for Adaptive Optics: the CAFADIS camera. We have obtained the atmospheric wavefront phase and the distance to two different laser guide stars. We have shown that the algorithms are time efficient for future giant telescopes requirements using specialized hardware as GPUs and FPGAs.

The robust and simple optical design of the CAFADIS camera will allow: wavefront and distance recovery, defocus correction, several LGS as reference, extended objects observation and tomographic wavefront sensing, all of that in a real time with a unique sensor. Future papers analyze these subjects. An study of this sensor has been included for the European Solar Telescopes (EST) Adaptive Optics. But the idea is also useful for nocturn telescopes.

Currently we envisage several applications for the plenoptic concept as a wavefront sensor for astronomical optics. Our most immediate goal is to refine the CAFADIS camera as a simultaneous sensor for the wavefront and focus from a Na LGS. Several aspects need to be improved with respect to what was discussed in the toy simulation presented in Section

3 as it was just intended to verify the conceptual feasibility of the plenoptic camera as a simultaneous wavefront and distance sensor. Currently, a more refined simulation is being designed which attempts to recover the distance from the fact the Na LGS is actually an extended 3D source and with a realistic simulation of signal-to-noise effects in CCD. We also need to understand the trade-offs between number of subapertures, number of pixels sampling each lenslet image and pixel scale at the CAFADIS CCD in order to optimize the simultaneous recovery of wavefront map and distance from the Na LGS. As pointed in Section 3, our hopes are that unlike with traditional wavefront sensors whose performances are degraded when considering extended sources, the CAFADIS camera is able to perform even better for the recovery of both the wavefront map and the height of the Na LGS. It is also important to notice that recovering the distance from the Na LGS using only its 3D nature is equivalent to determine the density profile of the mesospheric sodium layer.

However, we believe the potential of the plenoptic concept can be pushed further away as it could become the paradigm of wavefront sensing in astronomical optics. There are theoretical hints (Ziegler et Gross[15], (2007)) the plenoptic concept would be able to recover from a single LGS the whole turbulence volume sampled by the LGS photons. This opens up very exciting possibilities for the development of systems based on the plenoptic camera aiming at conducting tomography and multiconjugate adaptive optics.

7. ACKNOWLEDGMENTS

This work has been funded by "Programa Nacional I+D+i" (Project DPI 2006-07906) of the "Ministerio de Educación y Ciencia ", and by the "European Regional Development Fund" (ERDF).

REFERENCES

[1] R. M. Clare and R. G. Lane, "Wave-front sensing from subdivision of the focal plane with a lenslet array," JOSA A, Vol. 22, pp. 117-125, 2005.

[2] Rodríguez-Ramos, J.M., Magdaleno E., Domínguez Conde C., Rodríguez Valido M., and Marichal-Hernández J.G., "2D-FFT implementation on FPGA for wavefront phase recovery from the CAFADIS camera", SPIE Astronomical telescopes and instrumentation, Marseille, 2008.

[3] E. Adelson and J. Wang, "Single lens stereo with plenoptic camera", IEEE transactions on pattern analysis and machine intelligence, vol. 14, nº2, p. 99, 1992

[4] Ren Ng, "Fourier Slice Photography". Proceedings of SIGGRAPH, Los Ángeles (U.S.A.), 2005.

[5] Pérez Nava F., Marichal-Hernández J.G., Rodríguez-Ramos J.M., "The discrete focal stack transform", Eusipco, European Signal Processing Conference, Lausanne, 2008

[6] D. Summers, A. H. Bouchez, J. Chin, A. Contos, S. Hartman, E. Johansson, R. Lafon, D. Le Mignant, P. Stomski, M. A. van Dam, and P. L. Wizinowich, "Focus and pointing adjustments necessary for laser guide star adaptive optics at the W.M. Keck Observatory," in *Advancements in Adaptive Optics*, D. Bonaccini Calia, B. L. Ellerbroek, and R. Ragazzoni, eds., vol. 5490 of *Proc. SPIE*, pp. 1117–1128 (2004).

[7] M. E. Kasper, J. Charton, B. Delabre, R. Donaldson, E. Fedrigo, G. Hess, N. N. Hubin, J. Lizon, M. Nylund, C. Soenke, and G. Zins, "LGS implementation for NAOS," in *Advancements in Adaptive Optics*, D. Bonaccini Calia, B. L. Ellerbroek, and R. Ragazzoni, eds., vol. 5490, pp. 1071–1078 (2004).

[8] G. Herriot, S. Morris, S. Roberts, J. M. Fletcher, L. K. Saddlemayer, G. Singh, J. Véran, and E. H. Richardson, "Innovations in Gemini adaptive optics system design," SPIE **3353**, 488–499 (1998).

[9] M. Watanabe, H. Takami, N. Takato, S. Colley, M. Eldred, T. Kane, O. Guyon, M. Hattori, M. Goto, M. Iye, Y. Hayano, Y. Kamata, N. Arimoto, N. Kobayashi, and Y. Minowa, "Design of the Subaru laser guide star adaptive optics module," in *Advancements in Adaptive Optics*, D. Bonaccini Calia, B. L. Ellerbroek, and R. Ragazzoni, eds., vol. 5490 of *Proc. SPIE*, pp. 1096–1104 (2004).

[10] Sánchez-Blanco, E., GTCAO WFS design.

[11] G. Herriot, P. Hickson, B. Ellerbroek, J.P Véran, C.Y. She, R. Clare, D. Looze, (2006), "Focus errors from tracking sodium layer altitude variations with laser guide star adaptive optics for the Thirty Meter Telescope," in *Advances in Adaptive Optics II*, B. L. Ellerbroek, and D. Bonaccini Calia , eds., vol *Proc. SPIE* 6272 (2006).

[12] Davis, D.S., Hickson, P., Herriot, G, She, C.Y., "Temporal variability of the telluric sodium layer", Optics Letters, 31 (22), 3369 (2006)

[13] Carbillet, M., Vèrinaud, C., Femenía, B., Riccardi, A., Fini., L., "Modelling astronomical adaptive optics- I. The software package CAOS", MNRAS, 356, 12 (2005)

[14] Marichal-Hernández J.G. , Rosa F., Nava F.P., Rodríguez-Ramos J.M., "Fast discrete evaluation of plane integrals within an hypercube", to be submitted, 2008.

[15] Ziegler, R., Bucheli, S., Ahrenberg, L., Magnor, M., Gross, M."A Bidirectional Light Field - Hologram Transform" *EG 2007*